Appendix B: Validation and uncertainty information per IEC/IEEE 62704-2:2017 standard

The IEC/IEEE 62704-2 -2017 standard requires that the suitability of computational software be demonstrated, and that a number of uncertainty contributions be determined in order to determine the overall SAR simulation uncertainty.

Benchmarks have been defined in the standard for this purpose. In the following, the results of the required benchmark simulations are illustrated, and relevant uncertainty contributions evaluated. Subsequently, the overall simulation uncertainty is determined by adding the remaining uncertainty contributions.

The scope of this Appendix is limited, with few exceptions, to the antennas and frequency bands for which SAR simulations were required for the Motorola APX8500 all-band mobile radio. Both 1 g and 10 g SAR figures are reported in this Appendix to facilitate its global applicability. In order to obtain a single total-uncertainty figure for peak-spatial SAR, applicable to both 1g and 10g SAR, the higher of their contributions will be used in the root-sum-squared calculations.

Validation benchmarks for bystander and passenger exposure simulations

The benchmark models defined in the IEC/IEEE 62704-2:2017 standard were implemented using XFDTD™ v7.6 by Remcom, for bystander and passenger exposure conditions corresponding to standard simulation configurations, as required by the standard. The results showing the difference between the corresponding simulated SAR results and the standard reference values ("Ref") are listed in the tables below, for bystander and passenger, respectively, for 450 MHz.

SAR results computed for the bystander benchmark exposure configurations and the differences from the corresponding IEC/IEEE 62704-2:2017 standard reference values

Frequency, MHz	Antenna length, cm	1 g SAR, W/kg			10 g SAR, W/kg			WB SAR, W/kg		
		Ref	XFDTD	Delta, %	Ref	XFDTD	Delta, %	Ref	XFDTD	Delta, %
450	18	6.05E-03	5.71E-03	**-5.7%**	4.76E-03	4.68E-03	**-1.8%**	2.43E-04	2.37E-04	**-2.3%**

SAR results computed for the passenger benchmark exposure configurations and the differences from the corresponding IEC/IEEE 62704-2:2017 standard reference values

Frequency, MHz	Antenna length, cm	1 g SAR, W/kg			10 g SAR, W/kg			WB SAR, W/kg		
		Ref	XFDTD	Delta, %	Ref	XFDTD	Delta, %	Ref	XFDTD	Delta, %
450	18	1.38E-02	1.26E-02	**-9.0%**	9.24E-03	8.68E-03	**-6.0%**	5.46E-04	5.49E-04	**0.6%**

For all these results, the locations of the peak spatial-average SAR were the same as described in the Table C.2 of IEC/IEEE 62704-2 -2017 standard.

The maximum computed differences (highlighted cells) from the reference results across all evaluated benchmark configurations are 9.7% for the 1g SAR, 8.6% for the 10g SAR, and 4.9 % for the whole-body SAR. These differences are well within the expanded uncertainty of the simulations and therefore conform with the standard requirements for successful benchmark test.

Validation benchmarks and uncertainty of the human body model

The numerical validation of the standard human body model, and the corresponding uncertainty contribution, are presented herein. The bystander and passenger body models were simulated in the plane-wave exposure configurations defined in Clause 6.2 of the IEC/IEEE 62704-2 -2017 standard. The tables below show the standard reference SAR results together with the XFDTD SAR results in the corresponding validation configurations. The front and back impinging plane-wave exposure conditions are in the columns "Front" and "Back", respectively.

IEEE/IEC 62704-2:2017 standard reference and XFDTD SAR results for the bystander validation configurations

Bystander	Peak 1 g SAR, W/kg				Peak 10 g SAR, W/kg				Whole-body SAR, W/kg			
Frequency, MHz	Reference 62704-2		XFDTD		Reference 62704-2		XFDTD		Reference 62704-2		XFDTD	
	Front	Back	Front	Back	Front	Back	Front	Back	Front	Back	Front	Back
450	0.170	0.182	0.163	0.182	0.103	0.110	0.098	0.111	0.00628	0.00612	0.00626	0.00612

IEC/IEEE 62704-2:2017 standard reference and XFDTD SAR results for the passenger validation configurations

Passenger	Peak 1 g SAR, W/kg				Peak 10 g SAR, W/kg				Whole-body SAR, W/kg			
Frequency, MHz	Reference 62704-2		XFDTD		Reference 62704-2		XFDTD		Reference 62704-2		XFDTD	
	Front	Back	Front	Back	Front	Back	Front	Back	Front	Back	Front	Back
450	0.142	0.150	0.136	0.141	0.103	0.085	0.099	0.081	0.00485	0.00455	0.00480	0.00450

The tables below report the corresponding percental deviations of the XFDTD results from the standard reference results computed according to equation (8) of the IEC/IEEE 62704-2:2017 standard.

Percental difference between IEC/IEEE 62704-2:2017 standard references and XFDTD results for the bystander plane-wave validation configurations

Delta (XFDTD vs. Reference) for Bystander model						
Frequency, MHz	1 g SAR		10 g SAR		WB SAR	
	Front	Back	Front	Back	Front	Back
450	-4.03%	-0.10%	-4.18%	1.65%	-0.27%	-0.03%

Percental difference between IEC/IEEE 62704-2:2017 standard references and XFDTD results for the passenger plane-wave validation configurations

Delta (XFDTD vs. Reference) for Passenger model						
Frequency, MHz	1 g SAR		10 g SAR		WB SAR	
	Front	Back	Front	Back	Front	Back
450	-4.67%	-5.92%	-3.41%	-5.07%	-1.17%	-1.10%

Based on these results, the XFDTD peak spatial-average SAR values deviate from their respective reference results no more than 5.92% for the 1g SAR, 6.37% for the 10g SAR, while the whole-body average SAR deviates no more than 1.49%. Additionally, for all these results, the locations of the peak spatial-average SAR were the same as described in Table C.1 of IEC/IEEE 62704-2:2017 standard.

According to IEC/IEEE 62704-2:2017 standard, the above data constitute a successful validation of the human body numerical models, further yielding the relative uncertainty contributions to the overall numerical uncertainly budget.

Human body modeling uncertainty

Using the results presented above, the numerical human body model uncertainty contributions were derived for each frequency band based on the maxima of the respective deviations, separately for peak spatial-average SAR and the whole body-average SAR exposure conditions. They are summarized in the table below and will be subsequently used in determining the overall numerical uncertainty budget.

Uncertainty contributions of the numerical human body model

Frequency	450 MHz
Contribution to peak spatial-average SAR uncertainty	5.92%
Contribution to whole-body average SAR uncertainty	1.17%

Validation benchmark and uncertainty of the numerical vehicle model

The validation was performed implementing the numerical test configurations specifically defined for this purpose in Clause 6.2 of IEC/IEEE 62704-2:2017 standard. Accordingly, the magnitudes of the electric and magnetic fields were compared with the corresponding standard reference values computed in a set of predefined points outside and inside the vehicle, which are applicable to the bystander and passenger exposure conditions, respectively.

Validation for the Bystander Exposure Conditions

The tables below show the standard reference electric and magnetic field values and the corresponding XFDTD results computed in the validation configuration applicable to the bystander exposure conditions.

IEC/IEEE 62704-2:2017 standard reference and XFDTD electric field magnitude computed in the set of points defined for bystander test configurations

Point	Position above ground, cm	Electric field magnitude |E|, V/m					
		Reference 62704-2			XFDTD		
			450 MHz			450 MHz	
1	20		3.38E+00			3.79E+00	
2	40		3.12E+00			3.55E+00	
3	60		5.12E+00			5.97E+00	
4	80		6.13E+00			6.68E+00	
5	100		9.25E+00			1.01E+01	
6	120		1.16E+01			1.25E+01	
7	140		1.16E+01			1.24E+01	
8	160		1.02E+01			1.04E+01	
9	180		8.74E+00			8.67E+00	
10	200		7.83E+00			7.59E+00	

IEC/IEEE 62704-2:2017 standard reference and XFDTD magnetic field magnitude computed in the set f points defined for bystander test configurations

Point	Position above ground, cm	Magnetic field magnitude |H|, A/m					
		Reference 62704-2			XFDTD		
			450 MHz			450 MHz	
1	20		5.37E-03			5.83E-03	
2	40		1.07E-02			1.25E-02	
3	60		1.36E-02			1.54E-02	
4	80		1.55E-02			1.68E-02	
5	100		1.82E-02			1.87E-02	
6	120		3.21E-02			3.45E-02	
7	140		3.21E-02			3.47E-02	
8	160		2.67E-02			2.77E-02	
9	180		2.33E-02			2.27E-02	
10	200		2.08E-02			2.00E-02	

Based on these data, the deviations of XFDTD results from the respective reference values were computed according to equation (5) of IEC/IEEE 62704-2:2017 standard and are summarized in the following table.

Numerical vehicle modeling uncertainly contribution applicable to
1 g and 10 g peak spatial-average SAR in bystander exposure conditions

Frequency	450 MHz
Deviation	17.3%

The deviations in the above table are lower than the maximum 30% allowed in Clause 6.3.2 of IEC/IEEE 62704-2:2017 standard and successfully validate the numerical vehicle model used for the bystander exposure evaluations. These deviations are used to establish the uncertainty contribution from the numerical vehicle modeling applicable to 1 g and 10 g peak spatial-average SAR in the overall uncertainty budget.

In addition, the E and H field results were used to compute the numerical vehicle model uncertainty contribution to the whole-body average SAR estimate uncertainty. This contribution was computed according to equation (6) of the IEC/IEEE 62704-2:2017 standard and is summarized in the table below.

Numerical vehicle modeling uncertainly contribution applicable to
whole-body average SAR in bystander exposure conditions

Frequency	150 MHz	450 MHz	800 MHz
Deviation	18.3%	14.3%	15.0%

Validation for the Passenger Exposure Conditions

The following two tables show the standard reference electric and magnetic field values and the corresponding XFDTD results computed in the standardized validation configuration applicable to the passenger exposure conditions.

IEC/IEEE 62704-2:2017 standard reference and XFDTD electric field magnitude computed in the set of points defined for passenger test configurations

Point**Error! Bookmark not defined.**	Electric field magnitude |E|, V/m					
	Reference 62704-2			XFDTD		
		450 MHz			450 MHz	
1		1.87E+01			1.85E+01	
2		1.23E+01			1.27E+01	
3		9.08E+00			1.11E+01	
4		9.27E+00			7.63E+00	
5		1.32E+01			1.29E+01	
6		1.15E+01			9.84E+00	
7		1.27E+01			1.28E+01	
8		6.97E+00			7.51E+00	
9		6.41E+00			1.00E+01	

IEC/IEEE 62704-2:2017 standard reference and XFDTD magnetic field magnitude computed in the set f points defined for passenger test configurations

Point[1]	Magnetic field magnitude |H|, A/m					
	Reference 62704-2			XFDTD		
		450 MHz			450 MHz	
1		1.89E-02			2.14E-02	
2		2.57E-02			2.46E-02	
3		2.10E-02			2.36E-02	
4		2.68E-02			2.67E-02	
5		3.33E-02			3.53E-02	
6		3.34E-02			3.64E-02	
7		2.22E-02			2.09E-02	
8		2.44E-02			2.36E-02	
9		2.55E-02			1.76E-02	

[1] The points are defined in Table 14 of the IEEE/IEC 62704-2:2017 standard

Based on these data the deviations of XFDTD results from the respective references were computed according to equation (5) of IEC/IEEE 62704-2:2017 standard and are summarized in the table below.

Numerical vehicle modeling uncertainly contribution applicable to
1g and 10 g peak spatial-average SAR in passenger exposure conditions

Frequency	450 MHz
Deviation	30.4%

The deviations in the above table well below the maximum 45% allowed in Clause 6.3.2 of IEC/IEEE 62704-2:2017 standard and successfully validate the numerical vehicle model used for the bystander exposure evaluations. These deviations are used to establish the uncertainty contribution from the numerical vehicle modeling applicable to 1 g and 10 g peak spatial-average SAR in the overall uncertainty budget.

In addition, the E and H field results were used to compute the numerical vehicle model uncertainty contribution to the whole-body average SAR. This contribution was computed according to equation (6) of the IEC/IEEE 62704-2:2017 standard and is summarized in the table below.

Numerical vehicle modeling uncertainly contribution applicable to
whole-body average SAR in passenger exposure conditions

Frequency	450 MHz
Deviation	20.8%

Numerical vehicle modeling uncertainty

Using the results presented above, the numerical vehicle modeling uncertainty contributions for the UHF frequency bands were evaluated, separately for peak spatial-average SAR and the whole body-average SAR exposure conditions, based on the respective maxima of computed deviations. They are summarized in the table below, and will be subsequently used in determining the overall numerical uncertainty of SAR evaluations.

Frequency	450 MHz
Contribution to 1 g and 10 g peak spatial-average SAR uncertainty	30.4%
Contribution to whole-body average SAR uncertainty	20.8%

Uncertainty budgets

The overall uncertainty of the SAR evaluations depends on a number of uncertainty components:

a) numerical human body model,
b) numerical model of the vehicle,
c) numerical algorithm, and
d) numerical model of the antenna.[2]

The first two of these four components were determined in the foregoing. The remaining two are derived in the following, for the VHF, UHF, and 7/800 MHz frequency bands.

Numerical algorithm uncertainty

Table 3 in IEEE/ IEC 62704-1:2017 standard allows computing the numerical algorithm uncertainty on the basis of six uncertainty components:

a) positioning,
b) mesh resolution,
c) absorbing boundary conditions (ABCs),
d) power budget,
e) convergence, and
f) phantom dielectrics.

Two of these components, (b) and (f), are zero, as further explained here below.

The mesh resolution uncertainty component is zero since it is already accounted for by the other uncertainty components as noted in Clause 7.2.2 of IEC/IEEE 62704-2:2017 standard.

The phantom dielectrics uncertainty is zero since the dielectric parameters of the vehicle (PEC) and the phantom (tissues) are exactly specified and standardized.

The remaining components are determined as follows.

[2] The IEC/IEEE 62704-2:2017 standard requires the derivation of uncertainty contributions for antennas that differ from straight wires, while the uncertainty contributions for straight wire antennas is already included in the results evaluated according to Clause 7.2.3 of IEEE/IEC 62704-2.

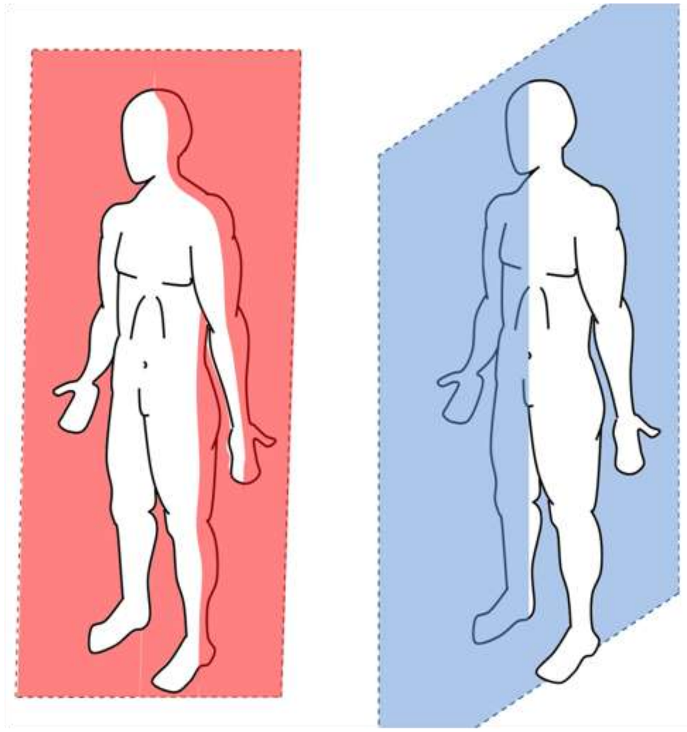

Coronal (left-hand side) and Sagittal (right-hand side) planes relative to the human body.

Positioning uncertainty

This uncertainty component is derived upon shifting the passenger and bystander models in the four directions defined by the model Sagittal and Coronal planes (assuming for simplicity the Coronal plane is orthogonal to ground also for the passenger) by a distance equal to the model resolution step (3 mm). The simulation setups for some frequency bands and exposures are shown in the following figures. For the sake of clarity, the offsets relative to the Coronal plane are called *front* and *back*, relative to the each model forward-facing direction, in the following. Similarly, shifts relative to the Sagittal plane are named *left* and *right* relative to the each model forward-facing direction.

The 1 g, 10 g peak spatial-average and whole-body SAR values in these shifted conditions are compared with the ones corresponding to the initial positions in order to determine the deviations to be used in deriving the respective uncertainty contributions.

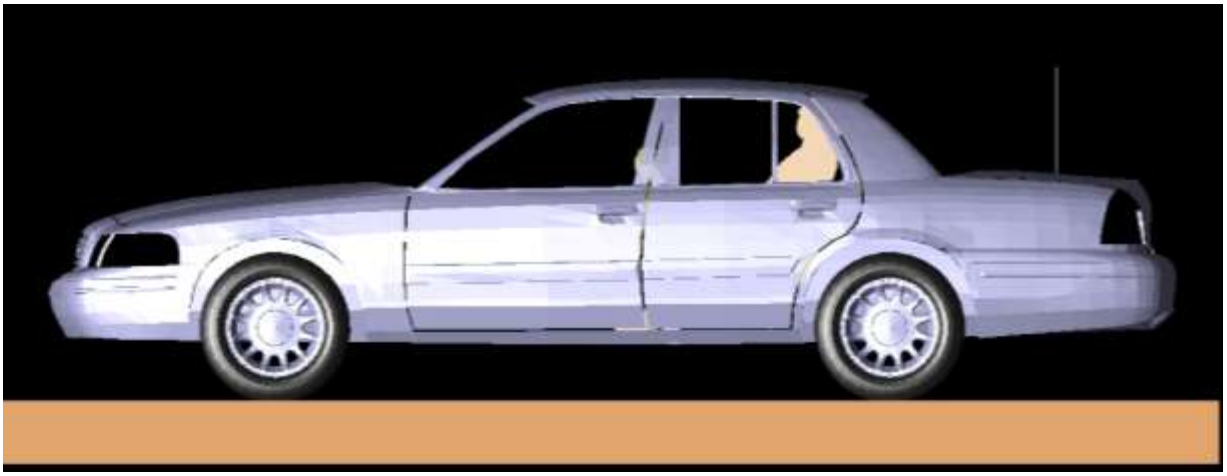

Passenger model in the center back-seat of vehicle equipped with a trunk-mount quarter-wave monopole antenna operating at VHF (150 MHz).

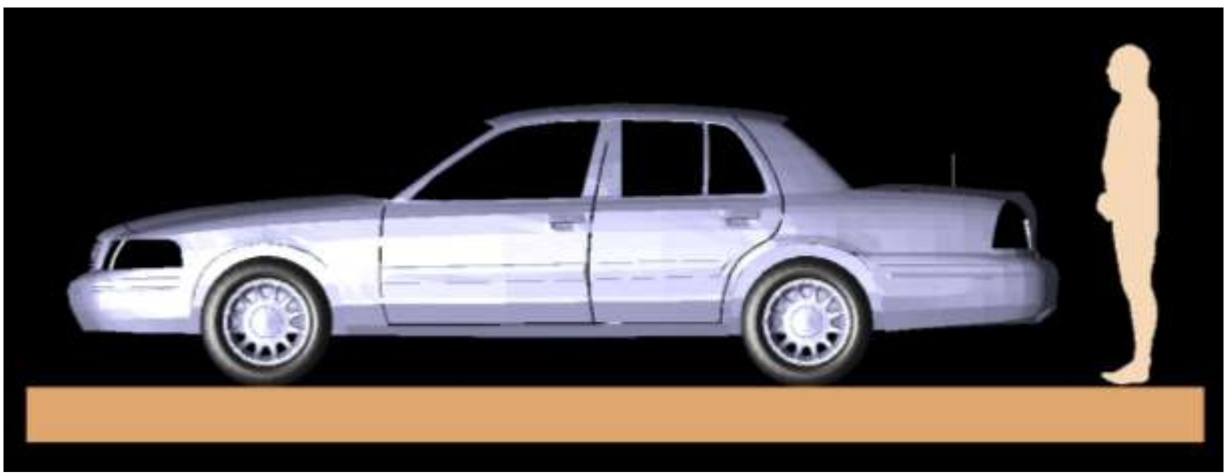

Centered bystander model at 20 cm from vehicle equipped with a trunk-mount quarter-wave monopole antenna operating at UHF (450 MHz).

The following table reports the initial SAR values in all three bands.

Initial SAR values normalized to 1 W net input power	450 MHz		
	1g	10g	WB
Bystander	7.34E-03	6.00E-03	3.60E-04
Passenger	1.26E-02	8.68E-03	5.49E-04

The two tables below report the SAR values computed for the different offset positions, and the percentage differences from the corresponding values in the initial positions.

SAR values normalized to 1 W net input power		450 MHz 1g	450 MHz 10g	450 MHz WB
Bystander 3 mm shift	front	7.26E-03	5.93E-03	3.61E-04
	back	7.23E-03	5.90E-03	3.56E-04
	right	7.33E-03	6.01E-03	3.60E-04
	left	7.31E-03	6.00E-03	3.60E-04
Passenger 3 mm shift	front	1.26E-02	8.82E-03	5.42E-04
	back	1.24E-02	8.61E-03	5.46E-04
	right	1.25E-02	8.68E-03	5.49E-04
	left	1.25E-02	8.68E-03	5.49E-04

Delta from initial SAR values, %		450 MHz 1g delta,%	450 MHz 10g delta,%	450 MHz WB delta,%
Bystander 3 mm shift	front	-0.6%	-0.7%	4.4%
	back	-1.1%	-1.2%	3.2%
	right	0.3%	0.6%	4.3%
	left	0.1%	0.3%	4.2%
Passenger 3 mm shift	front	0.4%	1.6%	-1.3%
	back	-1.1%	-0.9%	-0.6%
	right	-0.2%	-0.1%	-0.1%
	left	-0.2%	-0.1%	-0.1%

Taking the peak percental values highlighted above for each frequency band, irrespective of the local or whole-body SAR case or whether it is relative to passenger and bystander exposure, yields the uncertainty components to insert in Table 3 of the IEC/IEEE 62704-1:2017 standard: **4.4% for UHF**.

Absorbing boundary conditions uncertainty

This uncertainty component was computed by enlarging the computational domain by a quarter-wave separately in each of six directions (top, bottom, front, back, left, and right) relative to the front-facing car direction. This analysis was conducted for both the passenger and bystander exposure conditions described in the foregoing.

The following table reports the initial SAR values in all three bands.

Initial SAR values normalized to 1 W net input power	450 MHz		
	1g	10g	WB
Bystander	7.31E-03	5.98E-03	3.45E-04
Passenger	1.26E-02	8.68E-03	5.49E-04

The two tables below summarize the SAR values in the new conditions, and the percentage differences from the initial conditions.

SAR values normalized to 1 W net input power		450 MHz		
		1g	10g	WB
Bystander ABC expansion by $\lambda/4$	Back	7.31E-03	5.98E-03	3.46E-04
	Bottom	7.31E-03	5.98E-03	3.45E-04
	Front	7.08E-03	5.80E-03	3.45E-04
	Left	7.30E-03	5.97E-03	3.45E-04
	Right	7.30E-03	5.97E-03	3.45E-04
	Top	7.31E-03	5.98E-03	3.45E-04
Passenger ABC expansion by $\lambda/4$	Back	1.25E-02	8.68E-03	5.49E-04
	Bottom	1.26E-02	8.69E-03	5.49E-04
	Front	1.29E-02	8.72E-03	5.60E-04
	Left	1.26E-02	8.68E-03	5.49E-04
	Right	1.26E-02	8.68E-03	5.49E-04
	Top	1.26E-02	8.70E-03	5.49E-04

Delta from initial SAR values, %		450 MHz		
		1g delta,%	10g delta,%	WB delta,%
Bystander ABC expansion by $\lambda/4$	Back	0.00%	0.00%	-0.03%
	Bottom	-0.04%	-0.03%	0.00%
	Front	3.05%	3.00%	0.17%
	Left	0.04%	0.05%	0.00%
	Right	0.12%	0.13%	0.03%
	Top	-0.04%	-0.03%	0.03%
Passenger ABC expansion by $\lambda/4$	Back	0.16%	0.01%	-0.02%
	Bottom	0.00%	-0.08%	0.05%
	Front	-3.03%	-0.38%	-1.89%
	Left	0.00%	0.01%	-0.02%
	Right	0.00%	0.00%	-0.02%
	Top	-0.16%	-0.15%	0.00%

Taking the peak percental values highlighted above for each frequency band, irrespective of the local or whole-body SAR case or whether it is relative to passenger and bystander exposure, yields the uncertainty components to insert in Table 3 of IEC/IEEE 62704-1:2017 standard: **3.1% for UHF.**

Power budget uncertainty

This uncertainty component was derived by computing the forward and reflected power at the antenna feed-point, the RF power dissipated in the bystander or passenger and the pavement (vehicle and antennas are modeled as lossless metal), and the power radiated. The simulation results are normalized to a 1 W net (forward minus reflected) input power at the antenna feed-point. The following table reports the relevant RF power figures (rounded to the third significant digit), and the absolute percentage differences of the dissipated plus radiated power from the reference 1 W net input power.

Power figures in W	450 MHz	
	Bystander	Passenger
RF power forward	1.42E+00	1.37E+00
Net Power Accepted	1.00E+00	1.00E+00
Power Dissipated	4.38E-02	6.62E-02
Power Radiated	9.56E-01	9.34E-01
Power radiated + Power dissipated	1.00E-00	1.00E-00
|delta|, %	0.00%	0.00%

Based on this analysis, the uncertainty components to insert in Table 3 of IEC/IEEE 62704-1:2017 standard are negligible: **0.00% for UHF** bands.

Simulation convergence uncertainty

According to the IEC/IEEE 62704-1:2017 standard, simulations can be stopped when the long-term fluctuations of the squared E-field magnitude within the exposed subject are within 2% for time-harmonic simulations.

In reality, the long-term fluctuations in the SAR simulations included in this report are much smaller since a stringent convergence criterion was enforced. The typical level of convergence attained in these simulations is exemplified by reporting the long-term fluctuation levels for the simulation configurations analyzed so far to determine the algorithm uncertainty. This was done by placing E-field sensors in the head of the passenger, and in the torso of the bystander, as shown in the following figures.

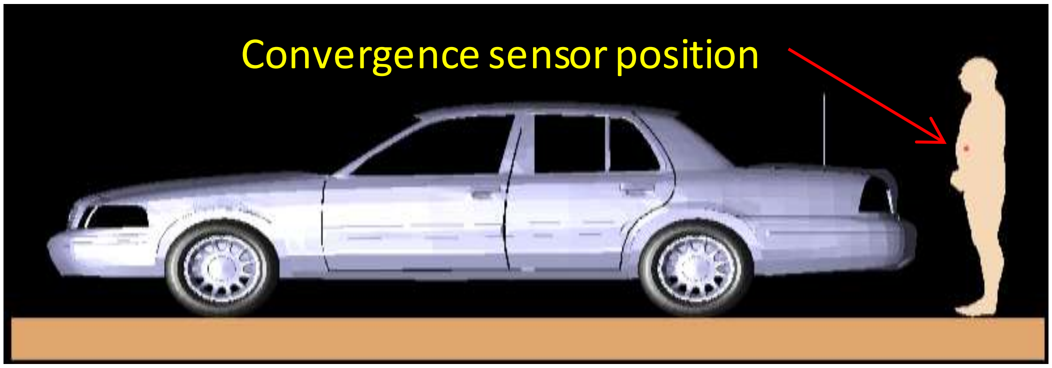

Location for the E-field sensors placed in the bystander for the convergence analysis.

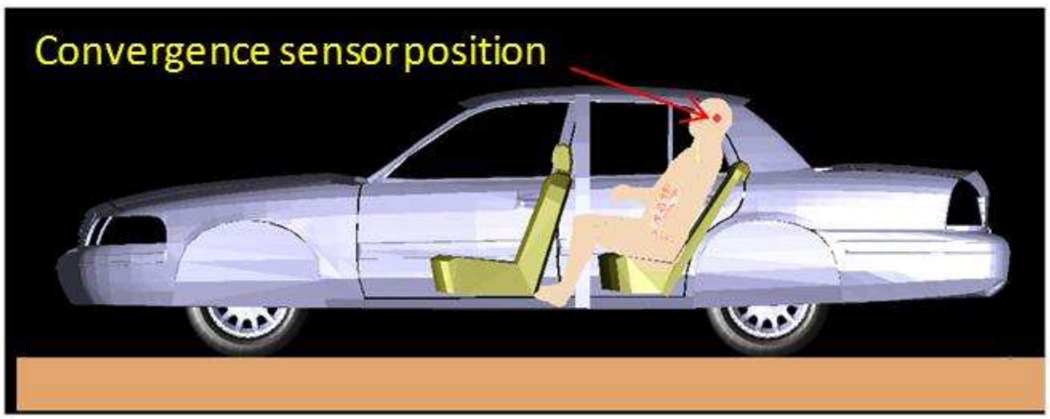

Locations for the E-field sensors placed in the passenger for the convergence analysis.

The following figures report the sensor E-field strength plots versus simulation time for the bystander and passenger configurations at UHF, spanning the entire duration of the simulations.

A portion of each plot is enlarged to highlight the levels of the last six E-field strength peaks. The corresponding values were then squared and tabulated, and the largest deviation computed and reported in the subsequent table.

For each band, the maximum deviation between bystander and passenger exposures is used as the uncertainty components of the simulation convergence.

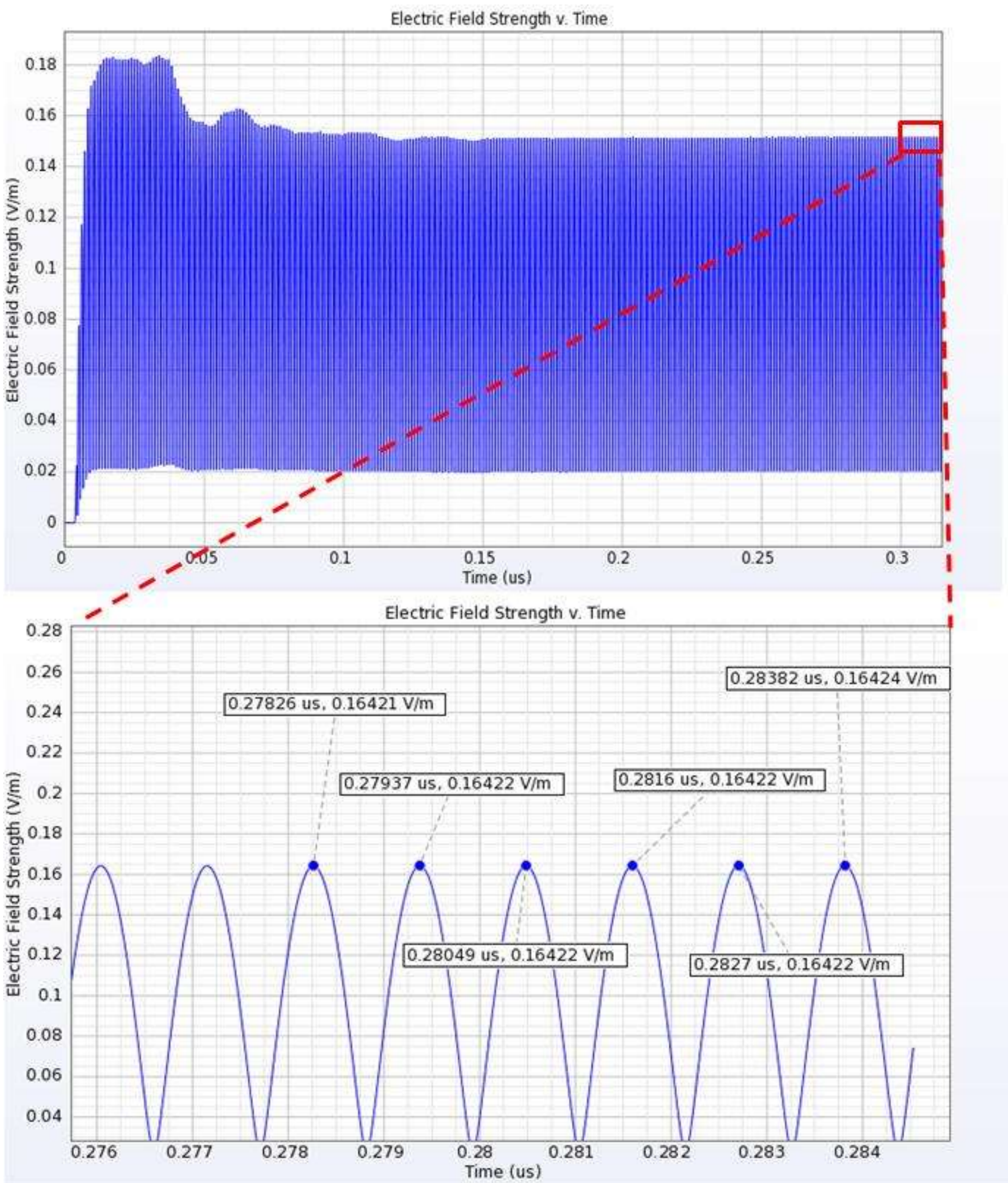

Sensor E-field strength vs. time used for the convergence analysis (bystander, 450 MHz).

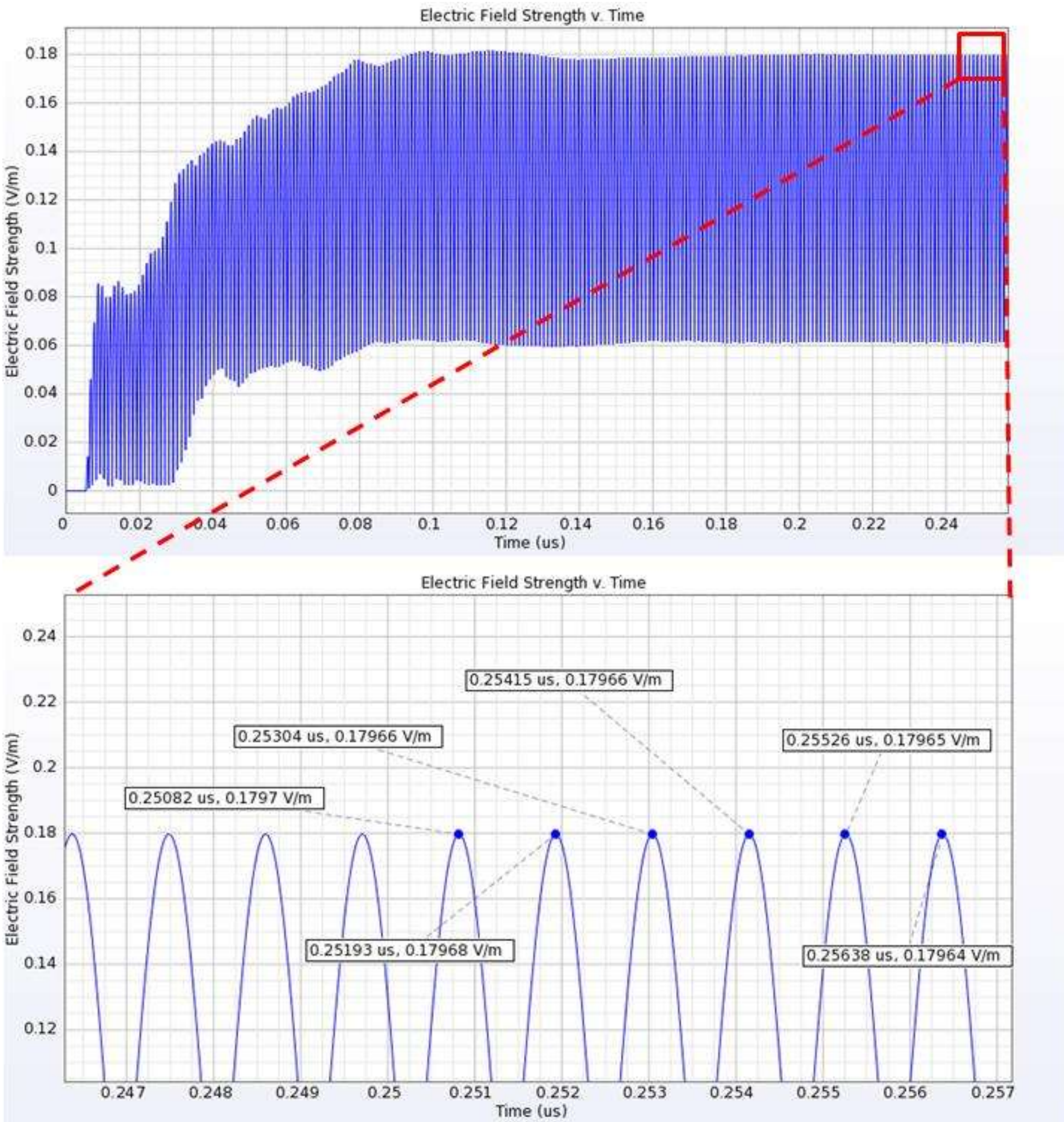

Sensor E-field strength vs. time used for the convergence analysis (passenger, 450 MHz).

Convergence analysis	450 MHz	
	Bystander	Passenger
|delta squared E-field|, %	0.02%	0.04%

Based on this analysis, the uncertainty components to insert in Table 3 of IEC/IEEE 62704-1:2017 standard (highlighted) are: **0.04% for UHF**

Algorithm uncertainty summary

Table 3 of IEC/IEEE 62704-1:2017 standard is replicated below to summarize the uncertainty components, and the respective divisors, and yield the **overall algorithm uncertainties at UHF (4.0%)**.

Budget of the uncertainty contributions of the numerical algorithm and of the rendering of the test- or simulation-setup (Table 3 from IEC/IEEE 62704-1:2017)

a	b	c			d	e	f	g		
Uncertainty component	**Subclause**	**Tolerance, %**			**Probability distribution**	**Divisor f(d,h)**	*ci*	**Uncertainty, %**		
			UHF						**UHF**	
Positioning	7.2.2		4.43		R	1.73	1		2.56	
Mesh resolution	7.2.3		0		N	1	1		0	
ABC	7.2.4		3.05		N	1	1		3.05	
Power budget	7.2.5		0.00		N	1	1		0.00	
Convergence	7.2.6		0.04		R	1.73	1		0.02	
Phantom dielectrics	7.2.7		0		R	1.73	1		0	
Combined standard uncertainty (*k* = 1)									**3.98**	

Uncertainty budgets

The overall numerical simulations uncertainty budget has been calculated according to Table 16 of IEC/IEEE 62704-2:2017 standard separately at at 450 MHz (UHF).

For simulations with antenna models representing straight wire monopoles, that being the case for all VHF and most UHF and 7/800 MHz antennas, no additional uncertainty contribution is required, as described in Clause 7.2.4 of IEC/IEEE 62704-2:2017 standard, since it is already included in the uncertainty of the numerical vehicle model. For the remaining antennas, a larger overall uncertainty must be computed to include their individual incremental uncertainty contributions. For this reason, uncertainty budgets are presented for wire antennas first, and then those of the remaining antennas are computed and presented in a separate table.

Uncertainty budgets for wire antennas

IEC/IEEE 62704-2:2017 standard numerical uncertainty budget for exposure simulations with vehicle mounted wire antennas and bystander and/or passenger model at 450 MHz (UHF)

a	*b*	*c*			*d*	*e* = *f*(*d*,*h*)	*f*	*g* = *c* × *f* / *e*			*h*
Uncertainty component	**Reference Clause**	**Deviation/ uncertainty**			**Prob. dist.**	**Div.**	c_i	**Standard uncertainty**			ν_{eff}
		1 g ± %	**10 g ± %**	**WB ± %**				**1 g ± %**	**10 g ± %**	**WB ± %**	
Numerical algorithm	7.2.2	–	–	–	–	–	–	4.0			–
Numerical model of the vehicle	7.2.3	30.4	30.4	20.8	R	√3	1	17.6	17.6	12.0	∞
Numerical model of antenna	7.2.4	0			R	√3	1	0			∞
SAR evaluation in the standard human body model	7.2.5	5.9	5.9	1.2	R	√3	1	3.4	3.4	0.7	∞
Combined standard uncertainty					RSS			**18.3**	**18.3**	**12.7**	∞
Expanded uncertainty					k = 2			**36.6**	**36.6**	**25.4**	

NOTE 1 Column headings *a* to *h* are given for reference.

NOTE 2 Abbreviations used in this table:

a) Div. — divisor used to get standard uncertainty. It is a function of probability distribution reported in column *d*, and degrees of freedom ν_{eff}, reported in column h;
b) 1 g, 10 g, and WB — uncertainty components of the peak spatial-average SAR for 1 g and 10 g, and the whole-body average SAR respectively;
c) R — rectangular probability distributions;
d) k — coverage factor;
e) c_i — sensitivity coefficient.

the sensitivity coefficient c_i is applied to convert each uncertainty component into the corresponding standard uncertainty for the SAR.

Uncertainty of the remaining antenna models

The uncertainty components for the remaining numerical antenna models were determined according to Clause 7.2.4 of IEC/IEEE 62704-2:2017 standard. The details for each antenna model validation are provided in the individual validation reports[3] accompanying this document. The corresponding uncertainty figures[4] evaluated according to equation (7) of IEC/IEEE 62704-2:2017 standard and the combined uncertainly budget for simulations with those antenna models are summarized in the following table.

Uncertainty budgets for the non-wire numerical antenna models

Antenna model	Incremental deviations for numerical antenna models, %	Combined standard uncertainty of wire antennas, %		**Combined standard uncertainty, %**		**Expanded uncertainty (k = 2), %**	
	1g/10g/WB	1g/10g	WB	1g/10g	WB	1g/10g	WB
HAE4011A	17.5	18.3	12.7	**21.0**	**16.3**	**42.0**	**32.6**

[3] The validations reports for those specific antenna models are provided in conjunction with this Appendix B as separate PDF file.

[4] These uncertainty figures are based on the individual incremental deviations evaluated for the numerical antenna models according to IEC/IEEE 62704-2:2017 standard and feature rectangular probability distribution.